Biochar physico-chemical properties as affected by environmental exposure

Science of the Total Environment xxx (2015) xxx–xxx

Contents lists available at ScienceDirect

Science of the Total Environment

journal homepage: www.elsevier.com/locate/scitotenv

# Biochar physico-chemical properties as affected by environmental exposure

Giovambattista Sorrenti [a,*], Caroline A. Masiello [b], Brandon Dugan [c], Moreno Toselli [a]

[a] Department of Agricultural Sciences, University of Bologna, viale G. Fanin 44, 40127 Bologna, Italy
[b] Departments of Earth Science, BioSciences, and Chemistry, Rice University, Houston, TX 77005, USA
[c] Department of Earth Science, Rice University, Houston, TX 77005, USA

## HIGHLIGHTS

- Porosity and surface chemistry control many biochar-induced environmental services.
- Ageing increased biochar skeletal and envelope density, but not porosity.
- Changes in hydrologic behaviors were linked to surface changes.
- Environmental exposure increased surface at% of O, S, N, Na, Al, Ca, Mn and Fe.
- Oxidation included the development of O-containing functional groups down to 75 nm.

## GRAPHICAL ABSTRACT

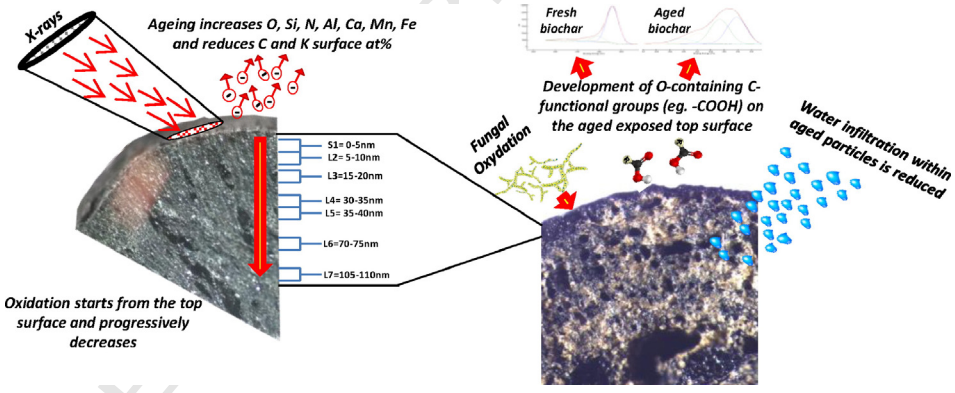


## ARTICLE INFO

*Article history:*
Received 5 February 2016
Received in revised form 25 March 2016
Accepted 26 March 2016
Available online xxxx

*Keywords:*
Charcoal
Density
Porosity
Imbibition
XPS
Ageing

## ABSTRACT

To best use biochar as a sustainable soil management and carbon (C) sequestration technique, we must understand the effect of environmental exposure on its physical and chemical properties because they likely vary with time. These properties play an important role in biochar's environmental behavior and delivery of ecosystem services. We measured biochar before amendment and four years after amendment to a commercial nectarine orchard at rates of 5, 15 and 30 t ha$^{-1}$. We combined two pycnometry techniques to measure skeletal ($\rho_s$) and envelope ($\rho_e$) density and to estimate the total pore volume of biochar particles. We also examined imbibition, which can provide information about soil hydraulic conductivity. Finally, we investigated the chemical properties, surface, inner layers atomic composition and C1s bonding state of biochar fragments through X-ray photoelectron spectroscopy (XPS). Ageing increased biochar skeletal density and reduced the water imbibition rate within fragments as a consequence of partial pore clogging. However, porosity and the volume of water stored in particles remained unchanged. Exposure reduced biochar pH, EC, and total C, but enhanced total N, nitrate-N, and ammonium-N. X-ray photoelectron spectroscopy analyses showed an increase of O, Si, N, Na, Al, Ca, Mn, and Fe surface (0–5 nm) atomic composition (at%) and a reduction of C and K in aged particles, confirming the interactions of biochar with soil inorganic and organic phases. Oxidation of aged biochar fragments occurred mainly in the particle surface, and progressively decreased down to 75 nm. Biochar surface chemistry changes included the development of carbonyl and carboxylate functional groups, again mainly on the particle surface. However, changes were noticeable down to 75 nm, while no significant changes were measured in the deepest

* Corresponding author.
*E-mail addresses:* g.sorrenti@unibo.it (G. Sorrenti), masiello@rice.edu (C.A. Masiello), dugan@rice.edu (B. Dugan), moreno.toselli@unibo.it (M. Toselli).

http://dx.doi.org/10.1016/j.scitotenv.2016.03.245
0048-9697/

layer, up to 110 nm. Results show unequivocal shifts in biochar physical and chemical properties/characteristics over short (~years) timescales.



## 1. Introduction

Biochar is the solid residue of biomass pyrolysis intentionally added to soil to sequester carbon (C) (Woolf et al., 2010), to ameliorate soil properties (Spokas et al., 2012) and to improve crop performance (Verheijen et al., 2010). Many biochar-induced ecosystem services, including improving soil water properties and ions retention, are due to its high (~75%) porosity which indicates the fraction of the total fragment volume not filled by solid (Brewer et al., 2014). Interconnected biochar pores are arranged in complex structures (Nguyen et al., 2010) and range from <1 nm (Sun et al., 2012; Keiluweit et al., 2010;) to pores on the order of 0.01 mm in size, reflecting the cellular arrangement of the pyrolyzed feedstocks (Bird et al., 2008; Wildman and Derbyshire, 1991) Pore surface area and reactivity control biochar sorptive capacities and modulate its interactions with minerals, water, microbes, fungal hyphae and plant roots (Downie et al., 2009; Thies and Rillig, 2009; Chen et al., 2008; Warnock et al., 2007; Hockaday et al., 2006; Pietikäinen et al., 2000). Recent findings suggest that pores >50 nm (nm) are responsible for most of the biochar porosity (Brewer et al., 2014). This result has been validated using mercury porosimetry by Baltrėnas et al. (2015) who estimated that up to 90% of either birch or pine-derived biochar pore volume consisted of pores larger than 500 nm in diameter while pores <500 nm took <1.5% of the total pore volume. Similarly, Laine and Yunes (1992) report than activated charcoal micropore surface area is larger than macropore surface area, but macropore volumes can be more than double than micropore volume. Macropores affect hydraulic conductivity (Masiello et al., 2015; Barnes et al., 2014; Brockhoff et al., 2010; Oguntunde et al., 2008) and other hydrologic processes (e.g. infiltration, erosiveness, wettability, water retention, nutrient leaching) (Baronti et al., 2014; Bruun et al., 2014; Novak et al., 2012; Major et al., 2009). These properties impact microbial habitats (Lehmann et al., 2011), offering shelters for mycorrhizal fungi (Warnock et al., 2007).

Biochar physico-chemical properties may change after environmental exposure, challenging our ability to predict its long-term ecosystem services. Changes result from shifts in temperature, water content, tillage, fertilization and interactions with the soil matrix (Joseph et al., 2010). Density and porosity of biochar can be altered through the trapping of minerals, roots, OM or microbes (Jaafar et al., 2014; Warnock et al., 2007), shifting biochar sorption capacity, soil hydraulic conductivity and water retention. (Masiello et al., 2015; Baronti et al., 2014).

Several studies report changes of biochar properties as a consequence of ageing (LeCroy et al., 2013; Lin et al., 2012; Jones et al., 2012; Joseph et al., 2010; Zimmerman, 2010; Cheng et al., 2008) However, most of these findings come from environmental exposures <-6 months or weathering induced through chemical and/or physical treatments (Yao et al., 2010).

Similarly, some studies suggest that oxidation is a surface process; others report oxidation throughout particles (Cheng et al., 2006). It seems reasonable to assume that chemical changes start at the surface, but no information exists about the progression of the oxidation front.

We evaluated porosity shifts induced by 4 years of environmental exposure by comparing fresh (never applied to the field) and field-applied biochar from the same biochar batch. We combined two pycnometry techniques to determine skeletal ($\rho_s$) and envelope ($\rho_e$) densities which allow estimation of porosity of biochar particles (Brewer et al., 2014). We also evaluated hydrologic implications of biochar ageing by an imbibition assay. Finally, we measured chemical properties, surface, inner layers elemental composition and C1s bonding state of biochar through X-ray photoelectron spectroscopy (XPS). We hypothesized that i) environmental exposure generates physical-chemical changes of biochar fragments, ii) chemical changes are not limited to the top exposed surface iii) the extent of the changes may be rate-dependent and iv) ageing alter biochar-water interactions.

## 2. Materials and methods

### 2.1. Experimental site and biochar characteristics

A four-year experiment was carried out using a commercial nectarine (*Prunus persica* L., Batsch) orchard (Big Top/GF677) planted in 1997 with a density of 519 trees $ha^{-1}$ (3.5 × 5.5 m) located in the southeastern Italian Po Valley (Tebano, Ravenna, 44° 29′ N, 11° 78′E, 58 m a.s.l.) on a sandy-loam Inceptisol soil with pH = 8.08, organic matter (OM) = 10.6 g $kg^{-1}$, cation exchange capacity (CEC) = 13.0 meq 100 $g^{-1}$, and total N, available P, exchangeable K, Na, Ca, and Mg of 800, 8, 97, 37, 2347, and 109 mg $kg^{-1}$.

The area has a temperate sub-continental climate with cold winters and warm, humid summers ($T_{average}$ = 13.6 °C; $T_{highest}$ = 40.5 °C, $T_{lowest}$ = −4.1 °C). Annual precipitation ranged between 650 and 910 mm. Alleys were maintained with native grass species while tree rows were herbicided with glufosinate ammonium (DL-phosphinothricin). Trees were managed by pruning, thinning, fertilization, irrigation, and control of pest and disease according to regional guidelines (ICM, 2009). From May to August trees were drip-irrigated and yearly fertilized with 0.25 kg N $tree^{-1}$ (130 kg N $ha^{-1}$) as urea at petal fall.

The biochar we used was produced in a commercial slow-pyrolysis unit (Romagna Carbone snc, Bagnacavallo (RA), Italy) using cylindrical, vertical charcoal kiln of 8.14 $m^3$ (2.40 m diameter and 1.80 m height). We used non-contaminated chipped hardwood (peach and grapevine at the same rate (v $v^{-1}$) pruning wood) slowly pyrolyzed with continuous (150 min) heating from ambient temperature (heating rate of 10–15 °C $min^{-1}$), reaching the highest T of ~550 °C with a 30 min peak temperature hold time (Table S1). Charred fragments were allowed to cool to ambient conditions in the absence of $O_2$.

#### 2.1.1. Experimental design

In November 2009 we distributed biochar at the rates of 5, 15, and 30 t fresh weight (fw) $ha^{-1}$ according to a randomized experimental block design, with 5 replicates of 5 trees each, arranged in 4 consecutive tree rows, leaving 10 unamended meters between consecutive plots. Treatments were randomly distributed in each row with at least one replicate per biochar rate in each row. Biochar was distributed on a 35 $m^2$ area per experimental plot (2 m wide along the herbicided strip) and mixed into the first 20-cm soil depth (A horizon) by a disc harrow. Control samples of biochar (never field-applied, termed here "fresh") were hermetically stored in plastic bags four years.

#### 2.1.2. Biochar recovery

We randomly recovered (Nov-13) ~50 biochar fragments of different sizes from each replicate. To accomplish this we removed the first 3–5 cm depth of the soil layer and carefully collected fragments from the soil by forceps, avoiding manual contact or any physical damage to the particles. We sealed the particles in polyethylene bags and transported them to the laboratory in a portable refrigerator. A composed biochar sample of ~2.5 kg (never field-applied, termed here "fresh") from the same biochar batch (from a unique and homogenized heap of ~2 t) was stored in hermetically closed plastic bags of ~250 g ea. and maintained four years at room temperature, in a dry and dark place.



Please cite this article as: Sorrenti, G., et al., Biochar physico-chemical properties as affected by environmental exposure, Sci Total Environ (2015), http://dx.doi.org/10.1016/j.scitotenv.2016.03.245

After four years, a random subset of these stored fresh biochar fragments (~100 pieces) were isolated by forceps, transferred in several test tubes, then analyzed as the soil-recovered biochar fragments.

Particles were dried at 50 °C for 72 h, sieved to 1 mm and the surface of individual fragments (keeping each piece by forceps under a magnifying lens) was cleaned with a soft brush and rinsed twice with deionized water (DI-$H_2O$) to remove adhering soil. Fragments were not physically damaged during handling and drying.

### 2.2. Biochar physical changes as affected by the environmental exposure

#### 2.2.1. Skeletal density ($\rho_s$)

Skeletal density ($\rho_s$) is the mass of a particle divided by its volume and was determined by helium (He) pycnomentry. We measured the $\rho_s$ of ~0.1 g dry biochar mass per replicate (samples composed of about 5–6 fragments, with each piece smaller than 1 $cm^3$) using an AccuPyc 1340 (Micromeritics, Norcross, GA) fitted with a 1 $cm^3$ chamber (Brewer et al., 2014).

#### 2.2.2. Envelope density ($\rho_e$)

Envelope density ($\rho_e$) is the mass of a dry biochar sample divided by the volume of its non-wetting exterior measured if an "envelope" were placed around each individual particle (Brewer et al., 2014). We measured $\rho_e$ of biochar samples that were ~0.215 g (dry mass) per replicate (samples composed of about 8–9 fragments, with each piece smaller than 1 $cm^3$) using a Geopyc 1360 Envelope Density Analyzer (Micromeritics, Norcross, GA). Fragments were placed in a bed of DryFlo® granular medium (density of ~0.4 g $cm^{-3}$). Consolidation was achieved by continuous rotation and vibration of the cylindrical chamber as the piston was gradually pushed into the chamber until the stated 22 N force was reached (Brewer et al., 2014).

#### 2.2.3. Porosity

Q10 Porosity ($\varphi$) is a function of $\rho_e$ and $\rho_s$:

$$\varphi = \frac{v_e - v_s}{v_e} = 1 - \frac{{}^{m}/_{\rho_s}{}^{s}}{{}^{m}/_{\rho_e}} = 1 - \frac{{\rho_e}^{e}}{\rho_s}$$

$v_e$ and $v_s$ = envelope and skeletal volume and $m$ = mass.

### 2.3. Imbibition assay

We compared aged biochar recovered from the 30 t $ha^{-1}$ plots with fresh biochar particles. Samples were treated as described earlier and three pairs of fragments with similar weight (±0.04 mg) and shape were selected, rinsed (DI-$H_2O$), and oven-dried at 75 °C for 48 h. The last washing step was repeated 3 times to reduce sample hydrophobicity. Fragments were individually transferred into 75 mL glass tubes filled with DI-$H_2O$ and carefully placed on the water surface, allowing the fragments to float. Tubes were unsealed, never disturbed, and maintained at room temperature, allowing natural water infiltration. We recorded the sinking of each fragment until particles reached the bottom of the tubes. The amount of absorbed water in sunken fragments was determined by massing before and after drying at 105 °C (96 h).

### 2.4. Biochar chemistry changes following environmental exposure

#### 2.4.1. pH and electrical conductivity (EC)

Oven-dried (105 °C) samples were added to DI-$H_2O$ at a mass ratio of 1:20 and shaken 90 min at 120 rpm (Rajkovich et al., 2012). pH and EC were measured on the filtered surnatant under continuous stirring by a pH-meter (BasiC 20, Crison, Barcelona, Spain) and a conductometer (CDM210 Conductivity Meter, Radiometer Analytical, Copenhagen, DK).

#### 2.4.2. Total C, N and H content

We sampled 3 mg of ground biochar for total N and H and 0.1 mg for C determination by catalytic combustion (ECS 4010, Costech Analytical Technologies Inc.; Valencia, CA).

#### 2.4.3. KCl extractable $NO_3^-$N and $NH_4^+$–N

We extracted intact oven-dried biochar fragments using a 2 M KCl solution at a ratio of 1:20 (w $w^{-1}$). Samples were shaken for 90 min at 100 rpm by an orbital shaker and the filtered (Whatman 42) surnatant was analyzed by a continuous flow autoanalyzer (AA-3, Bran + Luebbe, Norderstadt, Germany).

#### 2.4.4. Biochar surface atomic composition

We analyzed three fragments per replicate by XPS for relative C, O, Si, N, Na, Al, Mg, P, K, Ca, Mn, and Fe atomic composition (at%) in the top 5 nm (Fig. 1) using a PHI Quantera XPS with a focused monochromatic Al Kα X-ray source for excitation at 1486.6 eV and 49.2 W. We performed high-resolution, low-intensity scans to focus on the C bonding environments with 40 scans. XPS spectra were analyzed using a nonlinear, least-squares curve-fitting program with a Gaussian — Lorentzian mixed function to optimize the spectra using MultiPak data analysis software (MultiPak V7.0.1, Ulvac-Phi, Inc.).

#### 2.4.5. Biochar inner layer at%

We compared fresh and aged (from 30 t $ha^{-1}$ plots) biochar fragments (4 replicates) for relative C, O, Si, N, and Al at% at four depths (S1 = 0–5 nm, L2 = 5–10 nm, L3 = 15–20 nm and L4 = 30–35 nm; Fig. 1).

Three additional fragments of fresh and aged biochars were used to determine the relative C, O, Si, N, and Al at% at additional depths (S1 = 0–5 nm, L5 = 35–40 nm, L6 = 70–75 nm and L7 = 105–110 nm; Fig. 1).

We calibrated the XPS assessing the etching depth by using a standard 100 nm tick of $SiO_2$ as a reference. The relative etching rate for C-containing compounds was extrapolated by a computer simulation (based on the exact etching rate for $SiO_2$) as compared with a spreadsheet provided by the manufacturer.

We deconvoluted the C1s region bonding state into component functional groups. The –C–C/–C–H/–C = C bonds exhibit the same binding energy (284.74 eV) and thus were considered together, while –C–O, –C = O and –COOH were targeted at 285.95, 287.18 and 288.56 eV.

## 3. Statistical analyses

Data were evaluated according to a randomized block design with 5 replicates. Data of XPS analyses at different fragment depths were evaluated as a factorial randomized block design with 2 factors: biochar age (2 levels) and layer (4 levels). When ANOVA showed statistical effects ($p \leq 0.05$), means were separated by Student-Newman-Keuls Test; when interaction between factors was significant, 2 times standard error of means was used as the minimum difference between two statistically different means (Saville and Rowarth, 2008). Data of the imbibition assay were submitted to repeated measures analysis of variance using PROC MIXED (Littell et al., 1998) in SAS 9.0 (SAS Institute Inc. Q11 Cary, NC, USA), with the fragment weight as covariant and a compound symmetry covariance structure.

## 4. Results and discussion

### 4.1. Biochar physical properties as affected by environmental exposure

#### 4.1.1. Density and porosity

Field exposure induced the most significant physical changes in biochar $\rho_s$ and $\rho_e$, which increased by 160 and 15 mg $cm^{-3}$, respectively (Fig. 2).

This increase in $\rho_s$ may be due to biochar particle breakage and mechanical stresses (e.g. freeze-thaw cycles) as recently evidenced by



Please cite this article as: Sorrenti, G., et al., Biochar physico-chemical properties as affected by environmental exposure, Sci Total Environ (2015), http://dx.doi.org/10.1016/j.scitotenv.2016.03.245

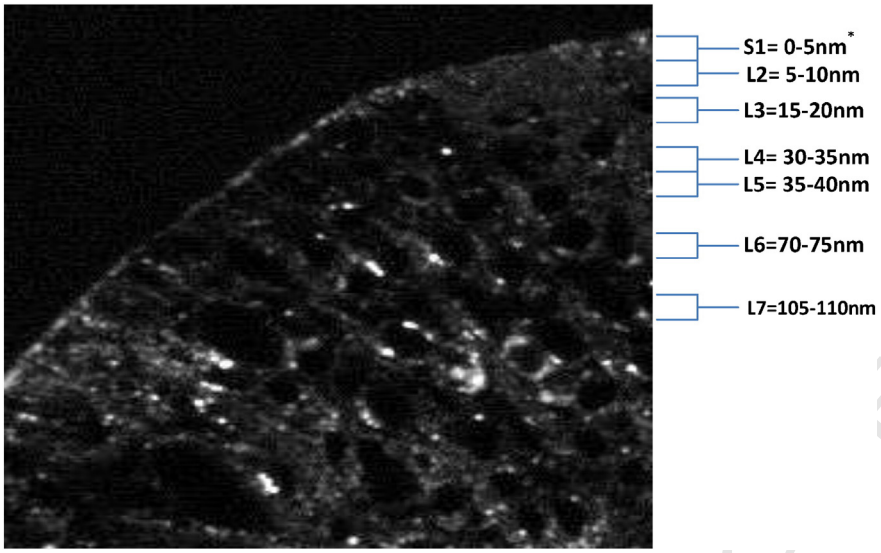


**Fig. 1.** The biochar profiles scanned by X-ray photoelectron spectroscopy (XPS). Magnification obtained by a Zeiss SteREO Discovery.V20 microscope. *Depths are not strictly to scale.

Spokas et al. (2014) who reported cracks and fractures (physical disintegration) on biochar surfaces induced by water and soil exposure. This breakage may increase pore connectivity by i) connecting previously isolated pores and ii) opening externally connected pores which may represent entry points for denser minerals that may fill or partially fill previously empty spaces. Similarly, capillary forces may also drive the soil solution into biochar pores since plant-derived biochars have a high concentration of macropores (>50 nm) (Downie et al., 2009), which are much larger than a water molecule (0.28 nm). Flowing water can carry small particles in suspension (including small biochar fragments) into biochar micropores; these particles may accumulate and/or clog in the pore channels (Joseph et al., 2010). Charred and non-charred compounds may remain physically blocked or chemically attracted within particles, altering pore connectivity (Jaafar et al., 2014; Joseph et al., 2010).

Recent studies support the rationale that soil particles (e.g. colloidal, dissolved, soluble inorganic salts and/or aluminosilicates) can fill exposed cavities of soil-exposed biochar fragments (Spokas, 2013; Spokas et al., 2014). Q12 Q13

Our microscopic images (Fig. 3) support the idea that interactions with minerals and/or microbes change the biochar's physical properties (Jaafar et al., 2014; Brodowski et al., 2006; Liang et al., 2006; Warnock et al., 2007; Hockaday et al., 2006) In our images minerals partially fill biochar fractures, starting from the particle's outer edges. Newly inaccessible volumes may be occupied by a combination of trapped water and/or air, leading to porosities that vary with water exposure history.

*4.1.2. Ageing reduced the rate of water imbibition*

Biochar pores have been classified as surface-site pores (α-type) and bulk-site pores (β-types) (Clarkson et al., 1998). As biochar become

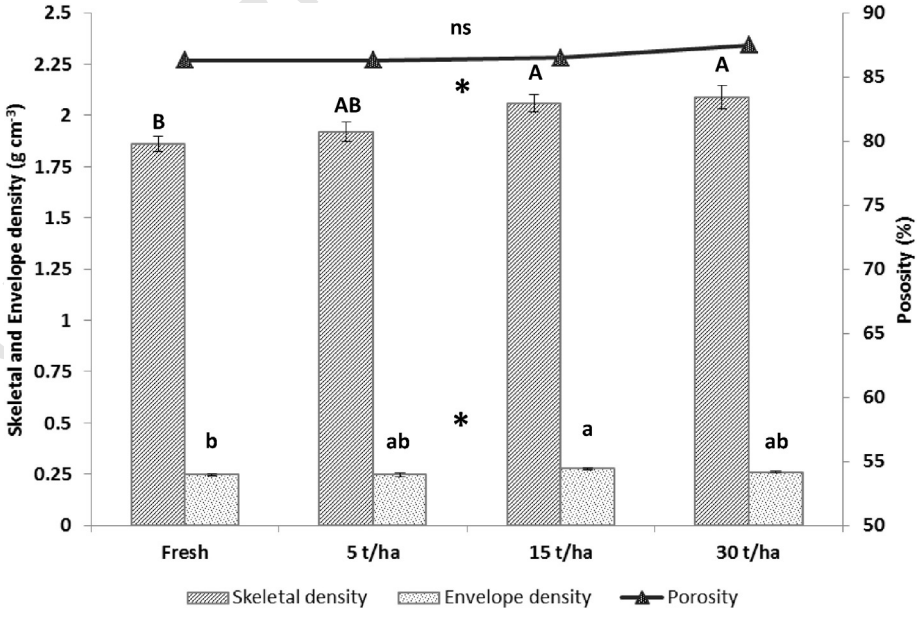


**Fig. 2.** Effect of environmental exposure (4 years in field conditions) on density (skeletal and envelope) and porosity of biochar fragments (avg. ± SE $n = 5$) applied at different rates as compared with fresh biochar. ns and * = effect of biochar ageing and rate not significant or significant at $p \leq 0.05$. Bars with the same letter are not statistically different ($p \leq 0.05$) according to the Student-Newman-Keuls (SNK) test.

Please cite this article as: Sorrenti, G., et al., Biochar physico-chemical properties as affected by environmental exposure, Sci Total Environ (2015), http://dx.doi.org/10.1016/j.scitotenv.2016.03.245

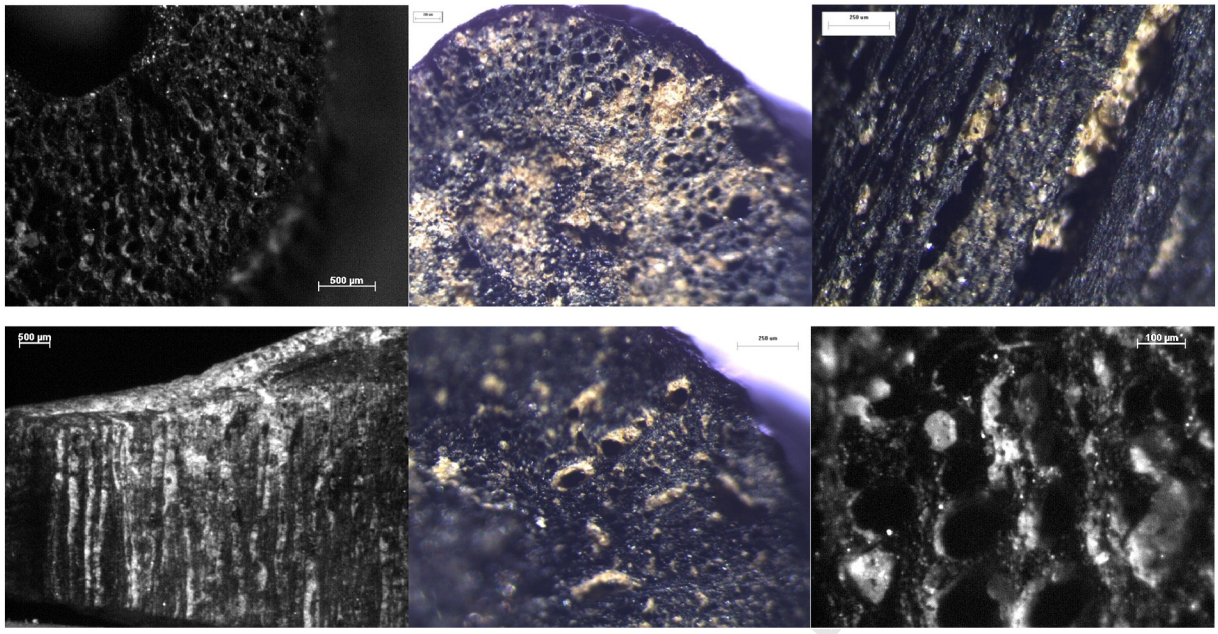


**Fig. 3.** Magnification of biochar fragments recovered from a nectarine orchard after 4 years of environmental exposure. Minerals and soil particles are adhering and/or are physically trapped over the entire particle surface. Pores appear partially or totally blocked by soil particles, likely reducing accessibility. Color magnifications were obtained by an Olympus SXZ16 microscope coupled with an Olympus digital camera whereas the others were obtained by a Zeiss SteREO Discovery.V20 microscope.

water-filled, diffusional processes allow the transition of water between the α-type and β-type pores. However, physical (pore size) and/or chemical (solid–liquid interactions) factors may interfere with water movement within biochar particles (Clarkson et al., 1998; Conte et al., 2013). When biochar pores totally or partially clog, water flow into and out of particles becomes physically hampered, hence water infiltration rate likely changes. In our biochar imbibition assay, fresh biochar sank faster than aged particles. Fresh biochar samples started to sink after 156 h and completely settled between 162 and 168 h while aged samples started sinking between 168 and 180 h, settling slowly up to 268 h, then accelerated until reaching the bottom of the tubes near 276 h (Fig. 4). The ratio of water:biochar (w $w^{-1}$) of the sunken fragments was unaffected by ageing and values were 4.98 (±0.30) and 5.16 (±0.35) for fresh and aged fragments, respectively. These results suggest that pore openings are becoming partially clogged, but not filled with solid materials.

However, as mentioned above, chemical factors may also interfere in the biochar-water relationship. This, in turn, refers to the development of H bonds between the water-derived O and H atoms of the biochar aromatic systems (Clarkson et al., 1998). The last interaction was elucidated by Conte et al. (2013), who suggested that water molecules may be bound to the solid carbonaceous material through non-conventional H bonds. As ageing induces the development of O– and H-containing functional groups onto the biochar surface, as a consequence of surface oxidation (Zimmerman, 2010), the last biochar-water mechanism results promoted in aged biochar with implications on the water mobility.

It seems also reasonable to hypothesize a similar reverse sense (pore drainage), with aged biochar fragments retaining water longer. In this case, and assuming water-saturated particles, the partial blocking of biochar pores may allow biochar-amended soils to hold water longer between rainfall events.

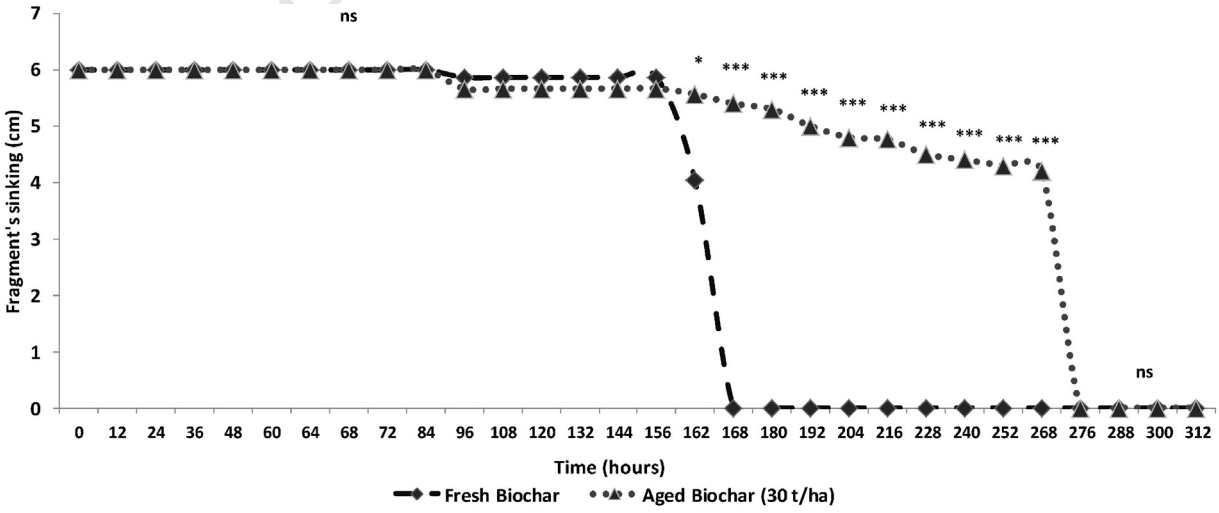


**Fig. 4.** Sinking dynamics of fresh vs. aged (4 years in field conditions at the rate of 30 t $ha^{-1}$) biochar fragments ($n = 3$). ns, * and *** = effect not significant or significant at $p \leq 0.05$ and $p \leq 0.001$, respectively.

Please cite this article as: Sorrenti, G., et al., Biochar physico-chemical properties as affected by environmental exposure, Sci Total Environ (2015), http://dx.doi.org/10.1016/j.scitotenv.2016.03.245

### 4.2. Biochar chemistry changes as affected by the environmental exposure

#### 4.2.1. pH, EC, total elemental C, N, H, extractable $NO_3^-$N and $NH_4^+$–N concentration

Ageing decreased biochar pH and increased EC (Table 1).

The weathering-induced carboxylic acids functional groups lead to a decrease of basic sites on the biochar surface (Qian and Chen, 2014; Yao et al., 2010; Cheng and Lehmann, 2009), explaining the significant reduction of pH (~2 units) in aged biochar. This suggests that biochar liming potential is be limited to few years after its application. Hence, biochar-induced benefits in nutrient availability in acid soils may be more pronounced in the first seasons following application. Similarly, the undesirable further pH increase in alkaline soils due to biochar application may be transient.

Total C concentration was reduced by 14.5% (±0.18) by ageing, irrespective of the application rate (Table 1). The last response is partly due to mineralization of the labile C-fraction associated with biochar (Norwood et al., 2013). This mineralization may occur through the loss of volatile organic compounds generated during pyrolysis and condensed during cooling (Rajkovich et al., 2012) which are more reactive than the aromatic fractions (Joseph et al., 2010). This leads to an initial evolution of biochar-derived $CO_2$ in soils after its application (few months), partly attributed to biochar surface oxidation (Bruun et al., 2008; Steiner et al., 2008).

Finally, a fraction of biochar-derived C was likely lost through leaching of dissolved organic C (DOC). Mukherjee and Zimmerman (2013), for instance, measured a significantly higher DOC in the soil leachate amended with two different biochars obtained at two pyrolysis temperatures. The additional rate of DOC in the leachate was unambiguously biochar-derived, as shown by the increase in the aromaticity of the DOC measured in the biochar-amended soil leachate (Barnes et al., 2014).

However, the 14% reduction of total C concentration in biochar fragments after 4 years soil incubation appear higher compared to mean averages reported in literature (Lehmann et al., 2009; Kuzyakov et al., 2014). To this regard, it must be mentioned that at the time of soil application, biochar was freshly produced thereby its content of water-soluble C-containing compounds was abundant, likely promoted also by the relatively low max T° (550 °C) reached during pyrolysis. In addition, a dilution effect induced by the attachment of organo-mineral complexes on the aged biochar surfaces is also reasonable, consistent with the increase of both the $N_{org}$ and $N_{min}$ fractions measured on the aged fragments. This last mechanism was recently proposed by Kammann et al. (2015) to explain $NO_3$–N capture on/in the porous biochar structure, encompassing with the development of acid and basic functional groups (as we also observed in our study) as well as the development of unconventional H-bonding.

Total N concentration increased in aged biochars by 3.8 fold, irrespective of application rate. Such increase was more pronounced when biochar was applied at 5 t $ha^{-1}$ (4.0 fold) and 30 t $ha^{-1}$ (4.2 fold) (Table 1). The most significant contribution to the total N increase was due to the organic N forms, which were 56% of the total N, on average. Similarly, Joseph et al. (2010) reported an increase in the N content of two different biochars mainly associated with proteins, amino acids, $NH_4^+$ and N–C compounds.

Likewise, extractable inorganic N increased in aged biochar, and $NO_3^-$ and $NH_4^+$ concentrations were significantly higher in aged than in fresh biochar, confirming the potential of charred biomasses in N retention and reduction in N-containing GHGs emission in soils (Spokas et al., 2012). However, recent evidences suggest that standard analytical methods (as adopted in our study) could not detect all biochar-bound nutrients, in particular nitrate-N, which may then remain frequently underestimated (Kammann et al., 2015). However, although the absolute total value we measured may be underestimated, the nitrate-N extracted from aged biochar (78.3 mg $kg^{-1}$) was 14 times higher than fresh biochar (5.5 mg $kg^{-1}$), and unlikely the total nitrate-N content of fresh biochar, would result higher than aged particles. Besides, Kammann et al. (2015) report that the non-detectable $NO_3$–N remains non-exchangeable and captured onto biochar particles, thereby we conclude that such portion is not available to plants.

#### 4.2.2. Biochar C and N behave differently as it ages in soil

Consistent with the total biochar C content (Table 1), XPS analyses showed that environmental exposure significantly reduced biochar C at% (Tables 2, 3 and Fig. 5).

Independent of the application rate, 4 years of field exposure reduced surface (0–5 nm) biochar relative C at% up to 35.5% compared to unexposed fragments (Fig. 5). The most intense reduction in biochar C at% occurred in the top 5 nm layer either in fresh (−13%) and aged biochars (−19.4%) (Table 2) as a response to the natural oxidation. Biochar C depletion was less intense in inner layers and no effects were observed in layers deeper than 35 nm in fresh particles. Depletion of C occurred up to 70 nm depth in aged fragments (Table 3). Within aged particles, biochar C at% vs depth could be fit by a positive regression model according to an exponential trend with a coefficient of determination ($R^2$) equal to 0.93 ($y = 44.025e^{0.1167x}$). These responses suggest that exposure in croplands strongly alters biochar C surface composition and that C depletion starts from the top exposed layer and proceed toward the interior, as a consequence of both biotic and abiotic oxidation. In our experiment after 4 years biochar's relative C content was reduced by ~15% compared to its initial values. This relative reduction in C content could be due to loss of biochar C, or it could simply be the result of increased contents of other atoms relative to C (Tables 2, 3), as mentioned above. Regardless, the amount of labile C lost compared to stable C stored in soils with biochar is still considered comparatively negligible and should not affect the C sequestration potential of biochar on a long-term basis (Joseph et al., 2010).

As expected, relative N at% was unaffected within layers of fresh particles (Tables 2 and 3). Total N concentration (Table 1) and N at% (Tables 2, 3 and Fig. 5) was statistically higher in aged fragments, showing the opposite trend compared to C. In aged fragments, biochar N at% was statistically higher mostly in the top surface (Fig. 5, Tables 2 and 3), up to 40 nm depth (Table 3). Ageing and depth significantly interacted with atomic N composition and it decreased progressively within aged fragments as the depth increased up to 75 nm depth (L6), while no differences were recorded between the deepest (L6 and L7) layers

**Table 1**
pH, electrical conductivity (EC), total C, H, N concentration and KCl extractable $NO_3$–N and $NH_4$–N of different rates of aged as compared with fresh biochar fragments.

| Biochar | pH | EC | C | H | N | $NO_3^-$N | $NH_4^+$–N |
|---|---|---|---|---|---|---|---|
| | | μS | g 100 $g^{-1}$ | g 100 $g^{-1}$ | g 100 $g^{-1}$ | mg $kg^{-1}$ | mg $kg^{-1}$ |
| Fresh | 9.97a | 903.5a | 77.6a | 1.41 | 0.23c | 5.51 b | 132.3 b |
| Aged 5 t $ha^{-1}$ | 7.81b | 129.8b | 66.7b | 1.48 | 0.92a | 82.5 a | 248.8 a |
| Aged 15 t $ha^{-1}$ | 8.09b | 144.8b | 66.3b | 1.40 | 0.73b | 69.2 a | 230.9 a |
| Aged 30 t $ha^{-1}$ | 8.08b | 158.2b | 66.1b | 1.21 | 0.97a | 83.4 a | 342.7 a |
| Significance | *** | *** | * | ns | *** | *** | ** |

ns, *, ** and *** = effect not significant or significant at $p < 0.05$, $p < 0.01$ and $p < 0.001$, respectively. In the same column, means followed by the same letter are not statistically different ($p < 0.05$, SNK Test).



Please cite this article as: Sorrenti, G., et al., Biochar physico-chemical properties as affected by environmental exposure, Sci Total Environ (2015), http://dx.doi.org/10.1016/j.scitotenv.2016.03.245

**Table 2**
Elemental composition (atomic concentration - at%) of aged (4-year in field conditions at 30 t ha$^{-1}$) biochar surface (S1) and 3 depths (L2, L3 and L4) compared with fresh biochar as determined by XPS.

| Ageing | C | N | | | | O | Al | Si |
|---|---|---|---|---|---|---|---|---|
| | | S1 (0–5 nm) | L2 (6–10 nm) | L3 (15–20 nm) | L4 (30-35 nm) | | | |
| Fresh | 91.6 | 1.2 | 0.89 | 0.85 | 0.76 | 6.7 | 0.29 | 0.47 |
| Aged | 55.3 | 3.15 | 1.40 | 1.15 | 1.13 | 32.7 | 3.73 | 6.50 |
| Significance | *** | | 2SEM = 0.50 | | | *** | *** | *** |
| DEPTH | | | | | | | | |
| S1 | 68.74 | | | | | 24.1 | 1.53 | 3.47 |
| L2 | 74.03 | | | | | 19.0 | 2.15 | 3.69 |
| L3 | 75.01 | | | | | 18.2 | 2.25 | 3.49 |
| L4 | 76 | | | | | 17.6 | 2.12 | 3.31 |
| Significance | ns | | | | | ns | ns | ns |
| Interaction | ns | | | ** | | ns | ns | ns |
| Ageing *Depth | | | | | | | | |

ns, ** and *** = effect not significant or significant at $p < 0.01$ and $p < 0.001$, respectively. Interaction between biochar and layer significant at $p < 0.01$. Values differing by ≥2 SEM are statistically differen.

(Table 3). This evidence suggests that mechanisms for N retention in aged biochar occur mainly in the exposed top surface, but are not only limited to this. Furthermore, the C/N ratio of the biochar fragments dramatically decreases as biochar ages, with potential implications for processes that are C/N-influenced (e.g. microbial activity).

*4.2.3. Environmental exposure alters biochar surface K, Ca, Mn and Fe ratio*

Ageing significantly affected the biochar surface relative at% of K, Ca, Mn and Fe with no effects induced by the application rate (Fig. 5). No differences were detected for Mg and P at%. Surface relative K at% of aged biochar was reduced compared to fresh biochar up to 29.3 fold for the 30 t ha$^{-1}$ application rate (Fig. 5). On the contrary, surface at% of Ca, Mn, and Fe were higher in aged fragments, with no effects induced by the application rate (Fig. 5). The most abundant increase was measured for Ca which increased by 90 fold while Mn at% recorded a limited increase, although significant. It is worth mentioning that these changes are expressed as relative at%, which estimate the relative atomic abundance ratio among scanned elements instead of giving the absolute concentration. Biochar surface ageing-induced effects can be ascribed either to physical or chemical mechanisms. The surface of the weathered biochar particles was finely coated with soil and organic residues which appeared to adhere and/or be trapped in pores and fractures, partially explaining the higher concentration for most of the elements found on the biochar surface. Chemical mechanisms involved the high reactive charge density of the biochar surface (Van Zwieten et al., 2010), which has adsorption sites where cations, clay, and organic matter may be ionically or covalently bound, confirming the interaction of biochar with minerals and organic compounds in soils. This may also contribute to explaining the higher values of O at% recorded in aged fragments (Fig. 5). The potential of biochar to retain minerals directly on its surface (Glaser et al., 2002) increases the ability of biochar to retain nutrients in soils. Various combinations of Al, Si, C, Fe, and Ti, and trace amounts of Ca, Mg, Mn, K, Na, P, and S were found at the external surfaces of aged greenwaste biochar particles (Joseph et al., 2010). However, the lack of change in the P and Mg atomic surface composition found in this study indicates that this process is biochar-type and soil dependent. Different processes (dissolution, hydrolysis, carbonation, decarbonation, hydration, redox reactions) and several mechanisms (H-bonding, cation-bridging, covalent bonding and hydrophobic types of interactions) are involved in biochar weathering processes as a consequence of its interactions with OM, water, adsorption of dissolved organic (e.g. root exudates) and inorganic compounds and oxidation (Joseph et al., 2010). In particular, the significant decrease of K at% in aged biochar surfaces we observed (87% in average relative to the fresh particles) may be due to the dissolution of soluble salts and organic compounds (i.e. biopolymers and low molecular weight compounds) associated with charred particles which is among the first reactions upon biochar addition to soil (Joseph et al., 2010; Shinogi et al., 2003). This is also confirmed by the reduced EC that we measured in aged particles. The dissolution process may induce a rapid increase in the availability of water soluble cations in the soil layer, where biochar is incorporated, thus when high rates are applied, biochar may represent a consistent source of K, enough to fulfill plant requirement (according to the application rate, biochar type and crop) for the first 2–3 seasons after its incorporation. However, results from a column experiment showed that weathering reduced not only the content of K but also S, Ca, and P (Yao et al., 2010), suggesting that mineral release from charred materials is controlled by biochar characteristics and the environment.

*4.2.4. Ageing promotes biochar oxidation, Al and Si at%*

Although chemically induced biochar degradation starts before incorporation in soil as a result of the oxidation of exposed C rings with a high density of π-electrons (Contescu et al., 1998) and free radicals (Montes-Morán et al., 2004), only once in soil does biochar experience significant chemical weathering. In our experiment, ageing increased values of biochar O, Al, and Si at% (Fig. 5, Table 2). Ageing and depth did not interact in atomic O, Al, and Si composition and values of biochar O, Al, and Si at%, were comparable among layers (Tables 2 and 3). Nevertheless, depth affected atomic O composition, which was reduced as the depth increased (Table 3). Independently of the layer, values of O, Al, and Si always increased in aged biochar by 3, 5, and 18 fold, respectively (Table 3). Environmental exposure promoted fragment's

**Table 3**
Atomic concentration (at%) of aged (4-year in field conditions at 30 t ha$^{-1}$) biochar surface (S1) and 3 depths (L5, L6 and L7) compared with fresh biochar as determined by XPS.

| Ageing | C | | | | N | | | | O | Al | Si |
|---|---|---|---|---|---|---|---|---|---|---|---|
| | S1 (0–5 nm) | L5 (35–40 nm) | L6 (70–75 nm) | L7 (105–110 nm) | S1 (0–5 nm) | L5 (35–40 nm) | L6 (70–75 nm) | L7 (105–110 nm) | | | |
| Fresh | 79.0 | 90.2 | 91.0 | 91.2 | 1.02 | 0.82 | 0.76 | 0.80 | 10.3 | 0.64 | 0.33 |
| Aged | 50.4 | 52.8 | 65.5 | 69.2 | 3.81 | 2.14 | 1.18 | 1.13 | 30.1 | 3.51 | 5.93 |
| Significance | | | 2SEM = 4.82 | | | | 2SEM = 0.81 | | *** | *** | *** |
| DEPTH | | | | | | | | | | | |
| S1 | | | | | | | | | 28.0a | 1.69 | 3.16 |
| L5 | | | | | | | | | 21.2b | 2.33 | 3.51 |
| L6 | | | | | | | | | 16.4c | 2.03 | 2.89 |
| L7 | | | | | | | | | 15.3c | 2.23 | 2.98 |
| Significance | | | | | | | | | *** | ns | ns |
| Interaction | | | * | | | | * | | ns | ns | ns |
| Ageing*depth | | | | | | | | | | | |

ns, * and *** = effect not significant or significant at $p < 0.05$ and $p < 0.001$, respectively. In the same column, means followed by the same letter are not statistically different ($p < 0.05$, SNK Test). Interaction between biochar and depth significant at $p < 0.05$. Values differing by ≥2 SEM are statistically different.
Estimated depth layers: S1 (0–5 nm), L5 (35-40 nm), L6 (70-75 nm), L7 (105-110 nm).



Please cite this article as: Sorrenti, G., et al., Biochar physico-chemical properties as affected by environmental exposure, Sci Total Environ (2015), http://dx.doi.org/10.1016/j.scitotenv.2016.03.245

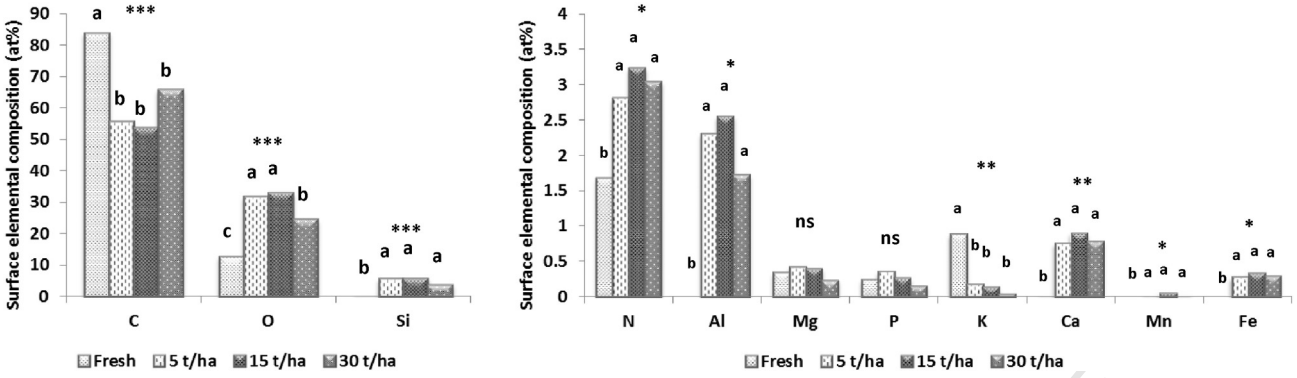


**Fig. 5.** Atomic percentage surface elemental composition (XPS) of aged (4 years) biochar applied at different rates as compared with fresh biochar. ns, *, ** and *** = effect of biochar ageing and rate not significant and significant at $p \le 0.05$, $p \le 0.01$ and $p \le 0.001$, respectively. Within each element, bars with the same letter are not statistically different ($p \le 0.05$), according to the Student-Newman-Keuls (SNK) test.

oxidation (Tables 2 and 3) and, independent of the age, oxidation started from the top exposed surface and was progressively reduced as depth increased down to 75 nm (Table 3), likely as a result of both biotic and abiotic processes, although some research suggests that biotic processes dominate (Zimmerman, 2010; Cheng et al., 2006). The O:C ratio of our biochar surface shifted from <0.074 to >0.58 after 4 years in field conditions as a consequence of the depletion of C and increase of O content. This may have consequences for biochar stability in soil, since the increase of the O:C ratio has been cited as a fundamental attribute in controlling the resistance to microbial mineralization (Harvey et al., 2012; Spokas et al., 2010;), although it may also simply reflect the increased O present in soil minerals and/or dissolved organic matter that have attached to the biochar.

#### 4.2.5. Oxidation affects biochar C functional groups

Our results show that biochar C functional groups were affected by the interaction between ageing and depth (Table 4). The relative at% of the C functional groups always increased by ageing in the top 3 layers (S1 + L5 + L6 layers, equal to 0–75 nm depth) (Table 4), except for the −C–C/–C–H/–C = C bonds, where only in the top surface an opposite trend was recorded (Table 4). No differences were measured in the deepest layer (105–110 nm) between fresh and aged biochars (Table 4). The overall development of C functional groups (–C = O, –C–O, –COOH) on the aged biochar surface as a consequence of the natural oxidation which involves the increase in O and H composition (Cheng et al., 2008; Yao et al., 2010; Jones et al., 2012; Lin et al., 2012; LeCroy et al., 2013; Qian and Chen, 2014) This oxidation is attributed to both biotic and abiotic processes, although some data suggest that biotic processes dominate (Cheng et al., 2006; Zimmerman, 2010). The increased oxidation of C in the uppermost surface layers of the aged biochar confirms that oxidation and/or adsorption of soil OM occurred (Joseph et al., 2010). Nevertheless, different functional groups can be formed on aged biochar through oxidation such as lactonic, o-quinone-like structures and ether-type oxygen (Boem, 2001). In our case, the –C-C/–C–H/C = C bonding state was always the major component of both fresh and aged biochar, although after 4 years the relative composition of these C bonds significantly decreased only in the top surface.

The most significant changes in the C1s bonding state were evident on the top surface (0–5 nm), where the relative concentration of –C = O, –C–O and, to a lesser extent, –COOH, were significantly higher in aged biochar. It is possible that carboxyl functional groups were less developed relative to other oxidized C forms because carboxyl groups may be partially decarboxylated through hydrolysis reactions occurring in solution (Yan et al., 1996).

### 4.3. Agronomical and ecological implications

Our findings suggest that biochar's effects on soil hydrology may change with time, raising a number of points. It seems reasonable to assume that different soil textures and mineralogies interact differently with various biochars; thus biochar and ecosystem-specific patterns of exterior pore blockage may be expected (Barnes et al., 2014). Furthermore, shifts in soil hydrology pose several implications for water-mediated processes as well as for the erosive fate of applied particles. For instance, soil leaching patterns may be different in aged biochar-mixed soils compared to the immediate response of biochar addition. Likewise, the influence of biochar on water retention may change as biochar ages, in particular in easily drained soils and especially if a dramatic reduction occurs in the number of pores between 0.01 and 0.1 mm. This pore-size range in biochar is fundamental to increased plant available water since larger pores weakly retain water under gravity (Jury et al., 1991) and smaller pores do not provide water in a plant-accessible form (Masiello et al., 2015).

**Table 4**
C1s bonding state and relative atomic percentage of aged (4-year in field conditions at 30 t $ha^{-1}$) biochar surface (S1) and 3 depths (L5, L3 and L7) compared with the fresh biochar as determined by XPS.

| Ageing | Binding energy (eV) (avg ± std dev) | | | | | | | | | | | | | | | |
|---|---|---|---|---|---|---|---|---|---|---|---|---|---|---|---|---|
| | −C–C/–CH/–C = C | | | | −C–O | | | | −C = O | | | | −COOH | | | |
| | *284.79* ± 0.05 | *284.76* ± 0.06 | *284.75* ± 0.04 | *284.75* ± 0.05 | *286.14* ± 0.46 | *285.96* ± 0.29 | *285.91* ± 0.21 | *285.85* ± 0.12 | *287.53* ± 0.5 | *286.91* ± 1.28 | *287.16* ± 0.61 | *287.19* ± 0.22 | *288.76* ± 0.39 | 288.87 ± 0.32 | *288.61* ± 0.45 | *288.73* ± 0.35 |
| | *S1* | *L5* | *L6* | *L7* | *S1* | *L5* | *L6* | *L7* | *S1* | *L5* | *L6* | *L7* | *S1* | *L5* | *L6* | *L7* |
| Fresh | 75.5 | 67.2 | 65.8 | 65.2 | 13.2 | 23.9 | 24.7 | 25.2 | 5.1 | 5.1 | 5.6 | 5.6 | 6.1 | 3.8 | 3.9 | 4.0 |
| Aged | 51.9 | 79.8 | 78.9 | 73.7 | 27.4 | 15.4 | 16.4 | 18.8 | 12.5 | 3.0 | 3.1 | 4.7 | 8.15 | 1.7 | 1.5 | 2.8 |
| Significance | 2SEM = 8.79 | | | | 2SEM = 7.35 | | | | 2SEM = 1.77 | | | | 2SEM = 1.29 | | | |
| Interaction ageing*depth | ** | | | | * | | | | *** | | | | * | | | |

*, ** and *** = Interaction between ageing and depth significant at $p < 0.05$, $p < 0.01$ and $p < 0.001$, respectively. Values differing by ≥2 SEM are statistically different.
Estimated depth layers: S1 (0–5 nm), L5 (35–40 nm), L6 (70–75 nm), L7 (105–110 nm).

Water infiltration shifts the functional density of biochar as water fills internal pores previously occupied by air. Once partially water-filled, the functional density of biochar particles exceeds that of water and the particles sink. The sinking process seems to be altered by field ageing, with mineral blockages of pore throats slowing the rate of water infiltration.

Similarly, it seems reasonable to hypothesize that it takes longer for aged fragments to dry out. This lag in particle infill time may suggest implications also for the erosion rate of biochar particles.

The porous structure of biochar provides suitable habitat for a range of microbial communities (Hockaday et al., 2006; Warnock et al., 2007; Downie et al., 2009; Thies and Rillig, 2009), and fungi can grow from within the pores out into the soil (Lehmann et al., 2011). Pore connectivity has been suggested to modulate the availability of biochar-associated labile organic compounds to microbial enzymes (Barnes et al., 2014). Easier access to these sites in recently added biochar could partially explain the initial high mineralization rates observed after biochar addition (Cross and Sohi, 2011). Our findings suggest potential shifts in microbial colonization patterns as biochar ages in soil. Due to ageing, the attachment of soil particles, changes in pore connectivity and pore clogging of biochar particles may alter habitat suitability and microbial activity (Lehmann et al., 2011; Thies and Rillig, 2009) reducing microbes colonization. However, fractures on the weathering particles may offer new opportunities for microbial colonization. Furthermore, minerals covering the external surface of biochar fragments interfere with its reactive surface, limiting its sorption capacity (Joseph et al., 2010) but at the same time the greater surface reactivity due to oxidation may promote physical protection of biochars and, thus, its long-term stability (Brodowski et al., 2006).

The development of O-containing C functional groups of aged biochar increases the reactivity of the biochar surface, leading to an enhancement of chemical sites able to retain nutrients and other organic compounds on this surface. This process is also responsible for the evolution of negative charges, raising the biochar CEC over time (Zimmerman, 2010).

These processes occurred mostly on the O-exposed biochar surface, leading to an enhancement of chemical sites able to retain nutrients and other organic compounds on this surface, consistent with the ion sorption pattern of our aged biochar. Oxidized biochar particles may then be bound to soil minerals. Mineral attachment has been indicated as one of the possible mechanisms for the slowing of biochar decomposition and oxidation (Brodowski et al., 2006; Nguyen et al., 2008), acting as a control on the stabilization process of charred particles.

Supplementary data to this article can be found online at http://dx.doi.org/10.1016/j.scitotenv.2016.03.245.

## Acknowledgments

We thank Dr. Xiaodong Gao and Dr. Bo Chen (Rice University, Houston, USA) for their valuable assistance with fragment density determinations and XPS analyses. We appreciated generous laboratory and equipment access provided by Dr. Helge Gonnermann. We also acknowledge funding from the US NSF through grants EAR 0911685 and 0949337. Authors thank three anonymous reviews for their valuable comments which helped to improve the manuscript.

## References

Baltrėnas, P., Baltrėnaitė, E., Spudulis, E., 2015. Biochar from Pine and Birch morphology and pore structure change by treatment in biofilter. Water Air Soil Pollut. 226 (3), 1–14.

Barnes, R.T., Gallagher, M.E., Masiello, C.A., Liu, Z., Dugan, B., 2014. Biochar-induced changes in soil hydraulic conductivity and dissolved nutrient fluxes constrained by laboratory experiments. PLoS One 9 (9), e108340.

Baronti, S., Vaccari, F.P., Miglietta, F., Calzolari, C., Lugato, E., Orlandini, S., Genesio, L., 2014. Impact of biochar application on plant water relations in *Vitis vinifera* (L.). Eur. J. Agron. 53, 38–44.

Bird, M.I., Ascough, P.L., Young, I.M., Wood, C.V., Scott, A.C., 2008. X-ray microtomographic imaging of charcoal. J. Archaeol. Sci. 35 (10), 2698–2706.

Boem, H.P., 2001. Carbon surface chemistry. In: Delhaes, P. (Ed.), Graphite and Precursors. CRC, Amsterdam, pp. 141–178.

Brewer, C.E., Chuang, V.J., Masiello, C.A., Gonnermann, H., Gao, X., Dugan, B., Driver, E.L., Panzacchi, P., Zygourakis, K., Davies, C.A., 2014. New approaches to measuring biochar density and porosity. Biomass Bioenergy 66, 176–185.

Brockhoff, S.R., Christians, N.E., Killorn, R.J., Horton, R., Davis, D.D., 2010. Physical and mineral-nutrition properties of sand-based turfgrass root zones amended with biochar. Agron. J. 102 (6), 1627–1631.

Brodowski, S., John, B., Flessa, H., Amelung, W., 2006. Aggregate-occluded black carbon in soil. Eur. J. Soil Sci. 57 (4), 539–546.

Bruun, S., Jensen, E., Jensen, L., 2008. Microbial mineralization and assimilation of black carbon: dependency on degree of thermal alteration. Org. Geochem. 39, 839–845.

Bruun, E.W., Petersen, C.T., Hansen, E., Holm, J.K., Hauggaard-Nielsen, H., 2014. Biochar amendment to coarse sandy subsoil improves root growth and increases water retention. Soil Use Manag. 30, 109–118.

Chen, B., Zhou, D., Zhu, L., 2008. Transitional adsorption and partition of nonpolar and polar aromatic contaminants by biochars of pine needles with different pyrolytic temperatures. Environ. Sci. Technol. 42 (14), 5137–5143.

Cheng, C.H., Lehmann, J., 2009. Ageing of black carbon along a temperature gradient. Chemosphere 75, 1021–1027.

Cheng, C.H., Lehmann, J., Thies, J.E., Burton, S.D., Engelhard, M.H., 2006. Oxidation of black carbon by biotic and abiotic processes. Org. Geochem. 37, 1477–1488.

Cheng, C.H., Lehmann, J., Engelhard, M.H., 2008. Natural oxidation of black carbon in soils: changes in molecular form and surface charge along a climosequence. Geochim. Cosmochim. Acta 72, 1598–1610.

Clarkson, R.B., Odintsov, B.M., Ceroke, P.J., Fruianu, M., Belford, R.L., 1998. Electron paramagnetic resonance and dynamic nuclear polarization of char suspensions: surface science and oximetry. Phys. Med. Biol. 43 (7), 1907.

Conte, P., Marsala, V., De Pasquale, C., Bubici, S., Valagussa, M., Pozzi, A., Alonzo, G., 2013. Nature of water-biochar interface interactions. GCB Bioenergy 5 (2), 116–121.

Contescu, A., Vass, M., Contescu, C., Putyera, K., Schwarz, J.A., 1998. Acid buffering capacity of basic carbons revealed by their continuous pK distribution. Carbon 36 (3), 247–258.

Cross, A., Sohi, S.P., 2011. The priming potential of biochar products in relation to labile carbon contents and soil organic matter status. Soil Biol. Biochem. 43 (10), 2127–2134.

Downie, A., Crosky, A., Munroe, P., 2009. Physical Properties of Biochar. In: Lehmann, J., Joseph, S. (Eds.), Biochar for Environmental Management: Science and Technology. Earthscan, London, pp. 13–32 (2009).

Glaser, B., Lehmann, J., Zech, W., 2002. Ameliorating physical and chemical properties of highly weathered soils in the tropics with charcoal—a review. Biol. Fertil. Soils 35, 219–230.

Harvey, O.R., Kuo, L.J., Zimmerman, A.R., Louchouarn, P., Amonette, J.E., Herbert, B.E., 2012. An index-based approach to assessing recalcitrance and soil carbon sequestration potential of engineered black carbons (biochars). Environ. Sci. Technol. 46, 1415–1421.

Hockaday, W.C., Grannas, A.M., Kim, S., Hatcher, P.G., 2006. Direct molecular evidence for the degradation and mobility of black carbon in soils from ultrahigh-resolution mass spectral analysis of dissolved organic matter from a fire-impacted forest soil. Org. Geochem. 37 (4), 501–510.

ICM, 2009. Integrated Crop Management. (http://agricoltura.regione.emilia-romagna.it/produzioni-agroalimentari/doc/disciplinari/produzione-integrata/archivio-dpi/disciplinari-di-produzione-integrata-2012. (Last visit October 1st, 2014)).

Jaafar, N.M., Clode, P.L., Abbott, L.K., 2014. Microscopy observations of habitable space in biochar for colonization by fungal hyphae from soil. J. Integr. Agric. 13 (3), 483–490.

Jones, D.L., Rousk, J., Edwards-Jones, G., DeLuca, T.H., Murphy, D.V., 2012. Biochar-mediated changes in soil quality and plant growth in a three year field trial. Soil Biol. Biochem. 45, 113–124.

Joseph, S., Camps-Arbestain, M., Lin, Y., Munroe, P., Chia, C.H., Hook, J., Van Zwieten, L., Kimber, S., Cowie, A., Singh, B.P., Lehmann, J., Foidl, N., Smernik, R.J., 2010. An investigation into reactions of biochar in soil. Aust. J. Soil Res. 48, 501–515.

Jury, W.A., Gardner, W.R., Gardner, W.H., 1991. Soil Physics. John Wiley & Sons, New York.

Kammann, C.I., Schmidt, H.P., Messerschmidt, N., Linsel, S., Steffens, D., Müller, C., Koyro, H.-W., Pellegrino, C., Stephen, J., 2015. Plant growth improvement mediated by nitrate capture in co-composted biochar. Sci. Rep. 5.

Keiluweit, M., Nico, P.S., Johnson, M.G., Kleber, M., 2010. Dynamic molecular structure of plant biomass-derived black carbon (biochar). Environ. Sci. Technol. 44 (4), 1247–1253.

Kuzyakov, Y., Bogomolova, I., Glaser, B., 2014. Biochar stability in soil: decomposition during eight years and transformation as assessed by compound-specific 14C analysis. Soil Biol. Biochem. 70, 229–236.

Laine, J., Yunes, S., 1992. Effect of the preparation method on the pore size distribution of activated carbon from coconut shell. Carbon 30, 601–604.

LeCroy, C., Masiello, C.A., Rudgers, J.A., Hockaday, W.C., Silberg, J.J., 2013. Nitrogen, biochar, and mycorrhizae: alteration of the symbiosis and oxidation of the char surface. Soil Biol. Biochem. 58, 248–254.

Lehmann, J., Czimczik, C., Laird, D., Sohi, S., 2009. Stability of biochar in soil. In: Lehmann, J., Joseph, S. (Eds.), Biochar for Environmental Management: Science and Technology. Earthscan, London, pp. 183–206 (2009).

Lehmann, J., Rillig, M.C., Thies, J., Masiello, C.A., Hockaday, W.C., Crowley, D., 2011. Biochar effects on soil biota—a review. Soil Biol. Biochem. 43 (9), 1812–1836.

Liang, B., Lehmann, J., Solomon, D., Kinyangi, J., Grossman, J., O'neill, B., Neves, E.G., 2006. Black carbon increases cation exchange capacity in soils. Soil Sci. Soc. Am. J. 70 (5), 1719–1730.

Lin, Y., Munroe, P., Joseph, S., Kimber, S., Van Zwieten, L., 2012. Nanoscale organo-mineral reactions of biochars in ferrosol: an investigation using microscopy. Plant Soil 357, 369–380.



Please cite this article as: Sorrenti, G., et al., Biochar physico-chemical properties as affected by environmental exposure, Sci Total Environ (2015), http://dx.doi.org/10.1016/j.scitotenv.2016.03.245

Littell, R.C., Henry, P.R., Ammerman, C.B., 1998. Statistical analysis of repeated measures data using SAS procedures. J. Anim. Sci. Biotechnol. 76 (4), 1216–1231.
Major, J., Steiner, C., Downie, A., Lehmann, J., 2009. Biochar effects on nutrient leaching. In: Lehmann, J., Joseph, S. (Eds.), Biochar for Environmental Management: Science and Technology. Earthscan, London, pp. 271–288.
Masiello, C.A., Dugan, B., Brewer, C.E., Spokas, K., Novak, J.M., Liu, Z., Sorrenti, G., 2015. Biochar effects on soil hydrology. In: Lehmann, J., Joseph, S. (Eds.), Biochar for Environmental Management: Science and Technology and Implementation, second ed. Routledg, London, pp. 541–560 (2009).
Montes-Morán, M.A., Suárez, D., Menéndez, J.A., Fuente, E., 2004. On the nature of basic sites on carbon surfaces: an overview. Carbon 42 (7), 1219–1225.
Mukherjee, A., Zimmerman, A.R., 2013. Organic carbon and nutrient release from a range of laboratory-produced biochars and biochar–soil mixtures. Geoderma 193, 122–130.
Nguyen, B.T., Lehmann, J., Kinyangi, J., Smernik, R., Riha, S.J., Engelhard, M.H., 2008. Long-term black carbon dynamics in cultivated soil. Biogeochemistry 89, 295–308.
Nguyen, B.T., Lehmann, J., Hockaday, W.C., Joseph, S., Masiello, C.A., 2010. Temperature sensitivity of black carbon decomposition and oxidation. Environ. Sci. Technol. 44 (9), 3324–3331.
Norwood, M.J., Louchouarn, P., Kuo, L.J., Harvey, O.R., 2013. Characterization and biodegradation of water-soluble biomarkers and organic carbon extracted from low temperature chars. Org. Geochem. 56, 111–119.
Novak, J.M., Busscher, W.J., Watts, D.W., Amonette, J.E., Ippolito, J.A., Lima, I.M., Gaskin, J., Das, K.C., Steiner, C., Ahmedna, M., Rehrah, D., Schomberg, H., 2012. Biochars impact on soil-moisture storage in an ultisol and two-aridisols. Soil Sci. 177, 310–320.
Oguntunde, P.G., Abiodun, B.J., Ajayi, A.E., van de Giesen, N., 2008. Effects of charcoal production on soil physical properties in Ghana. J. Plant Nutr. Soil Sci. 171, 591–596.
Pietikäinen, J., Kiikkila, O., Fritze, H., 2000. Charcoal as a habitat for microbes and its effect on the microbial community of the underlying humus. Oikos 89, 231–242.
Qian, L., Chen, B., 2014. Interactions of aluminium with biochars and oxidized biochars: implications for the biochar aging process. J. Agric. Food Chem. 62 (2), 373–380.
Rajkovich, S., Enders, A., Hanley, K., Hyland, C., Zimmerman, A.R., Lehmann, J., 2012. Corn growth and nitrogen nutrition after additions of biochars with varying properties to a temperate soil. Biol. Fertil. Soils 48 (3), 271–284.
Saville, D.J., Rowarth, J.S., 2008. Statistical measures, hypotheses, and tests in applied research. J. Nat. Resour. Life Sci. Educ. 37, 74–82.
Shinogi, Y., Yoshida, H., Koizumi, T., Yamaoka, M., Saito, T., 2003. Basic characteristics of low-temperature carbon products from waste sludge. Adv. Environ. Res. 7 (3), 661–665.
Spokas, K.A., 2013. Impact of biochar field aging on laboratory greenhouse gas production potentials. GCB Bioenergy 5 (2), 165–176.
Spokas, K., Baker, J., Reicosky, D., 2010. Ethylene: potential key for biochar amendment impacts. Plant Soil 333, 443–452.
Spokas, K.A., Cantrell, K.B., Novak, J.M., Archer, D.W., Ippolito, J.A., Collins, H.P., Boateng, A.A., Lima, I.M., Lamb, M.C., McAloon, A.J., Lentz, R.D., Nichols, K.A., 2012. Biochar: a synthesis of its agronomic impact beyond carbon sequestration. J. Environ. Qual. 41 (4), 973–989.
Spokas, K.A., Novak, J.M., Masiello, C.A., Johnson, M.G., Colosky, E.C., Ippolito, J.A., Trigo, C., 2014. Physical disintegration of biochar: an overlooked process. Environ. Sci. Technol. Lett. 1, 326–332.
Steiner, C., Glaser, B., Teixeira, W.G., Lehmann, J., Blum, W.E.H., Zech, W., 2008. Nitrogen retention and plant uptake on a highly weathered central amazonian ferralsol amended with compost and charcoal. J. Plant Nutr. Soil Sci. (Zeitschrift Fur Pflanzenernahrung Und Bodenkunde) 171, 893–899.
Sun, H., Hockaday, W.C., Masiello, C.A., Zygourakis, K., 2012. Multiple controls on the chemical and physical structure of biochars. Ind. Eng. Chem. Res. 51 (9), 3587–3597.
Thies, J., Rillig, M., 2009. Characteristics of biochar: Biological properties. In: Lehmann, J., Joseph, S. (Eds.), Biochar for Environmental Management: Science and Technology. Earthscan, London, pp. 85–106.
Van Zwieten, L., Kimber, S., Morris, S., Chan, K.Y., Downie, A., Rust, J., Joseph, S., Cowie, A., 2010. Effects of biochar from slow pyrolysis of papermill waste on agronomic performance and soil fertility. Plant Soil 327, 235–246.
Verheijen, F., Jeffery, S., Bastos, A.C., van der Velde, M., Diafas, I., 2010. Biochar application to soils: a critical scientific review of effects on soil properties, processes and functions. Joint Research Centre (JRC) Scientific and Technical Report No EUR 24099 EN. Office for the Official Publications of the European Communities, Luxembourg.
Warnock, D.D., Lehmann, J., Kuyper, T.W., Rillig, M.C., 2007. Mycorrhizal responses to biochar in soil: concepts and mechanisms. Plant Soil 300 (1–2), 9–20.
Wildman, J., Derbyshire, F., 1991. Origins and functions of macroporosity in activated carbons from coal and wood precursors. Fuel 70 (5), 655–661.
Woolf, D., Amonette, J.E., Street-Perrott, F.A., Lehmann, J., Joseph, S., 2010. Sustainable biochar to mitigate global climate change. Nat. Commun. 1, 56.
Yan, F., Schubert, S., Mengel, K., 1996. Soil pH increase due to biological decarboxylation of organic anions. Soil Biol. Biochem. 28, 617–624.
Yao, F.X., Arbestain, M.C., Virgel, S., Blanco, F., Arostegui, J., Macia-Agullo, J.A., Macias, F., 2010. Simulated geochemical weathering of a mineral ash-rich biochar in a modified Soxhlet reactor. Chemosphere 80, 724–732.
Zimmerman, A.R., 2010. Abiotic and microbial oxidation of laboratory-produced black carbon (biochar). Environ. Sci. Technol. 44 (4), 1295–1301.



Please cite this article as: Sorrenti, G., et al., Biochar physico-chemical properties as affected by environmental exposure, Sci Total Environ (2015), http://dx.doi.org/10.1016/j.scitotenv.2016.03.245